

Article

Effect of Methionine Oxidation and Substitution of α -Conotoxin TxID on α 3 β 4 Nicotinic Acetylcholine Receptor

Jie Ren ^{1,2}, Rui Li ¹, Jiong Ning ¹, Xiaopeng Zhu ¹, Dongting Zhangsun ¹, Yong Wu ¹ and Sulan Luo ^{1,*} 

¹ Key Laboratory of Tropical Biological Resources, Ministry of Education, Key Laboratory for Marine Drugs of Haikou, Hainan University, Haikou 570228, China; hndx2303@163.com (J.R.); flychcken@163.com (R.L.); ningjiong2018@163.com (J.N.); zhuxiaopeng@hainu.edu.cn (X.Z.); zhangsundt@163.com (D.Z.); wys211@163.com (Y.W.)

² Institute of Tropical Agriculture and Forestry, Hainan University, Haikou 570228, China

* Correspondence: luosulan2003@163.com; Tel./Fax: +86-0898-6628-9538

Received: 21 May 2018; Accepted: 15 June 2018; Published: 20 June 2018



Abstract: α -Conotoxin TxID was discovered from *Conus textile* by gene cloning, which has 4/6 inter-cysteine loop spacing and selectively inhibits α 3 β 4 nicotinic acetylcholine receptor (nAChR) subtype. However, TxID is susceptible to modification due to it containing a methionine (Met) residue that easily forms methionine sulfoxide (MetO) in oxidative environment. In this study, we investigated how Met-11 and its derivatives affect the activity of TxID using a combination of electrophysiological recordings and molecular modelling. The results showed most TxID analogues had substantially decreased activities on α 3 β 4 nAChR with more than 10-fold potency loss and 5 of them demonstrated no inhibition on α 3 β 4 nAChR. However, one mutant, [M11I]TxID, displayed potent inhibition at α 3 β 4 nAChR with an IC₅₀ of 69 nM, which only exhibited 3.8-fold less compared with TxID. Molecular dynamics simulations were performed to expound the decrease in the affinity for α 3 β 4 nAChR. The results indicate replacement of Met with a hydrophobic moderate-sized Ile in TxID is an alternative strategy to reduce the impact of Met oxidation, which may help to redesign conotoxins containing methionine residue.

Keywords: α -Conotoxin TxID; methionine oxidation and substitution; α 3 β 4 nAChR; peptide synthesis and activity assay; molecular dynamics simulations

1. Introduction

Conotoxins (Conopeptides, CTxs) are produced by marine cone snails belonging to the *Conus* genus, which are disulfide-constrained peptides targeting a range of ion channels and receptors [1–4]. α -CTxs are a subgroup of conotoxins characterized by their ability to inhibit nicotinic acetylcholine receptors (nAChRs) [5–8]. The nAChRs have been implicated in a range of diseases including pain, addiction, dementia, Parkinson’s disease, schizophrenia, obesity and cancer et al. [9,10]. As such, α -Ctxs are potential treatments for these difficult miscellaneous diseases.

A structurally novel α -conotoxin, TxID, was discovered by gene cloning in our lab from *Conus textile*. It consists of 15 amino acid residues possessing one readily oxidizable methionine at position 11 (Met-11) (Figure 1). TxID belongs to the α -4/6 conotoxin subfamily that potently blocks α 3 β 4 nAChR subtype with high selectivity [11]. Differential sensitivity of α -CTx TxID on stoichiometry of α 3 β 4 nAChR was examined previously. We used three α 3: β 4 RNA injection ratios of 1:1, 1:10 and 10:1 to form three different stoichiometry receptors of α 3 β 4 subtype [12]. The results showed that inhibition of 1:10 injection ratio by TxID was comparable with regular 1:1 α 3 β 4 nAChRs within

2-fold difference. However, potency of 10:1 injection ratio decreased 5-fold comparing with 1:1 $\alpha\beta4$ nAChR. TxID exhibited different sensitivity on different stoichiometry of $\alpha\beta4$ nAChRs, which could reflect different stoichiometries of α and β subunit [12]. To better understand which amino acids are responsible for the activity of TxID, we performed alanine scanning mutagenesis on all residues except for four Cys residues. TxID completely lost its inhibitory activity at $\alpha\beta4$ nAChR when five residues (i.e., His-5, Pro-6, Val-7, Met-11 and Pro-13) were mutated to alanine respectively. For [G1A]TxID, activity decreased nearly 19-fold relative to wild-type peptide. Other analogues, [S4A]TxID, [S9A]TxID, [S12A]TxID and [I14A]TxID almost maintained full potency at $\alpha\beta4$ nAChR. Our homology models and molecular dynamics(MD) simulations suggested that critical residues His-5, Pro-6 and Val-7 in loop 1 of TxID interacted with the $\alpha3$ subunit, whereas Met-11 and Pro-13 located in loop 2 are close to $\beta4$ subunit [11,13]. These results reveal that Met is one of critical residues for binding $\alpha\beta4$ nAChR.

Methionine and cysteine are the only two sulfur-containing proteogenic amino acids and are extremely vulnerable to oxidation *in vivo*. Cystines are oxidized to form disulfide bonds that are crucial for structural and biological function of proteins. Oxidation of the amino acid methionine generates methionine sulfoxide (MetO) which may play a vital role in mediating the physiological function of some proteins [14]. With this information in mind, we investigated whether the oxidation of Met to MetO could alter the potency of α -CTx TxID at $\alpha\beta4$ nAChR subtype. Additionally, Met residue was substituted by other amino acids to ascertain the impact of position 11 on TxID activity (Figure 1). In a series of electrophysiological experiments, we accessed activities of these analogues at various nAChR subtypes. Using electrophysiology assays combined with computer dynamic stimulations, we hoped to reveal the molecular mechanism of Met acting with $\alpha\beta4$ nAChR subtype.

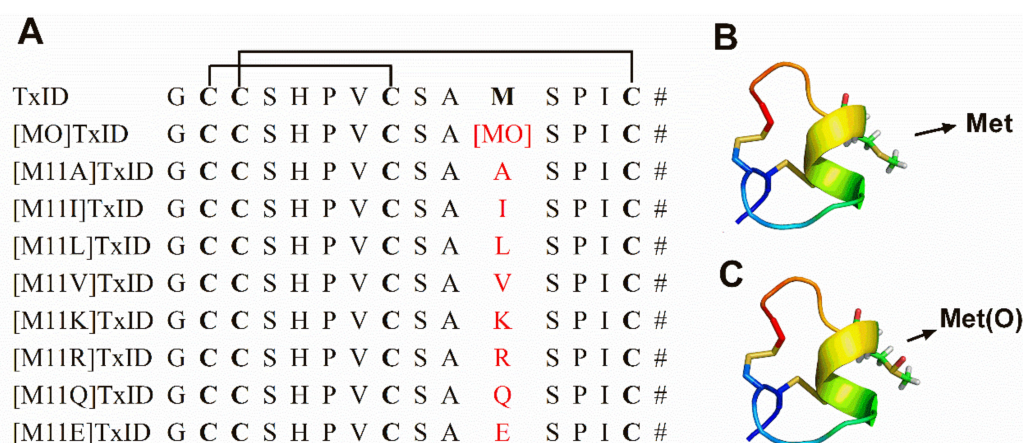


Figure 1. Sequences alignment of α -CTx TxID analogues with Cys (I-III, II-IV) disulfide bond connectivity (A) and structures of TxID (B) and [MO]TxID (C). (A) The sequences of TxID analogues are shown and the substituted residues at position 11 are highlighted in red. The # indicates an amidated C terminus; (B) Structural representation of TxID (PDB ID code 2M3I); (C) Spatial structure of [MO]TxID while Met residue is oxidized to MetO by addition of oxygen to its sulfur atom, which was produced by PyMOL.

2. Results

2.1. Peptide Synthesis

The native TxID and its derivatives were synthesized using Fmoc solid phase peptide synthesis with the side chains of Cys residues protected in pairs. Cys I and Cys III were protected by the acid-labile trityl (Trt) while Cys II and Cys IV were protected by the acid-resistant acetamidomethyl (Acm) [14]. Disulfide bonds with Cys (I-III, II-IV) connectivity of these peptides were formed using two-step oxidations. The folded peptide of TxID and its analogues were purified by HPLC.

Electrospray-mass spectroscopy confirmed molecular mass of the folded peptides which was consistent with their corresponding theoretical values.

The [MO]TxID was synthesized through 10% hydrogen peroxide (H_2O_2) oxidation according to the reaction scheme of Methionine (TxID) + 10% $H_2O_2 \rightarrow$ Methionine Sulfoxide (TxID) + H_2O . Then the oxidative product was purified by RP-HPLC. When methionine of TxID was oxidized to sulfoxide methionine, the hydrophilicity of [MO]TxID increased remarkably and its retention time shifted from 15.48 min to 11.42 min (Figure 2A,C). Meanwhile, the molecular weight of TxID and [MO]TxID was determined by ESI-MS respectively (Figure 2B,D). [MO]TxID showed a molecular weight increase of 16 Da, which was consistent with its theoretical mass (Figure 2B,D).

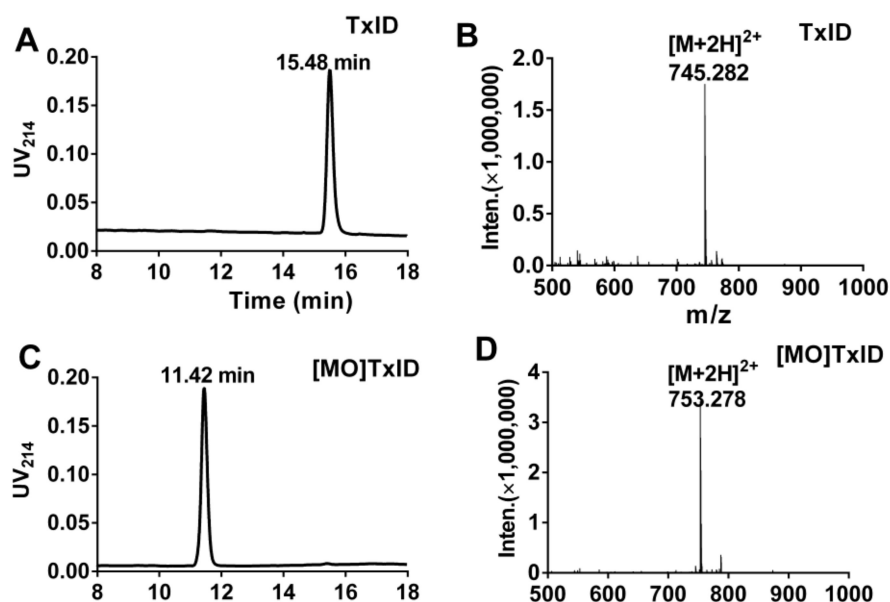


Figure 2. HPLC chromatograms and mass spectra of α -CTx TxID and [MO]TxID. Peptides were analyzed on a reversed phase analytical Vydac C18 (5 μ m, 4.6 mm \times 250 mm) HPLC column using a linear gradient of a 10–40% buffer B, and 90–60% buffer a over 20 min, where B = 0.05% TFA in 90% ACN; a = 0.075% TFA in water. The elution profile was monitored by measuring the absorbance at 214 nm. (A) HPLC chromatogram of α -CTx TxID; (B) Electrospray ionization mass spectrometry (ESI-MS) data for TxID with observed monoisotopic mass of 1488.56 Da; (C) HPLC chromatogram of [MO]TxID; (D) ESI-MS data for [MO]TxID with an observed monoisotopic mass of 1504.56 Da.

2.2. Characterization of [MO]TxID Effect on the $\alpha 3\beta 4$ nAChR Subtype

The influence of Met oxidation of TxID on $\alpha 3\beta 4$ nAChR subtype expressed in *Xenopus* oocytes was investigated. Representative traces of TxID and [MO]TxID on $\alpha 3\beta 4$ nAChR are shown in Figure 3. At a concentration of 1 μ M, TxID almost blocked 100% of ACh-evoked $\alpha 3\beta 4$ nAChR-mediated currents whereas [MO]TxID only inhibited 72% of current amplitude (Figure 3A,B). At a concentration of 100 nM, TxID caused potent blockade of ACh-evoked currents (~80%), but [MO]TxID only inhibited 25% of current amplitude (Figure 3C,D). The concentration response curves indicated that TxID inhibited $\alpha 3\beta 4$ nAChR with an IC_{50} of 18 nM (Figure 3E, Table 1). Remarkably, the IC_{50} value of [MO]TxID was 245 nM which was almost 13.3-fold less potent than that of TxID (Figure 3E, Table 1). These findings demonstrate that methionine is essential for TxID binding rat $\alpha 3\beta 4$ nAChR.

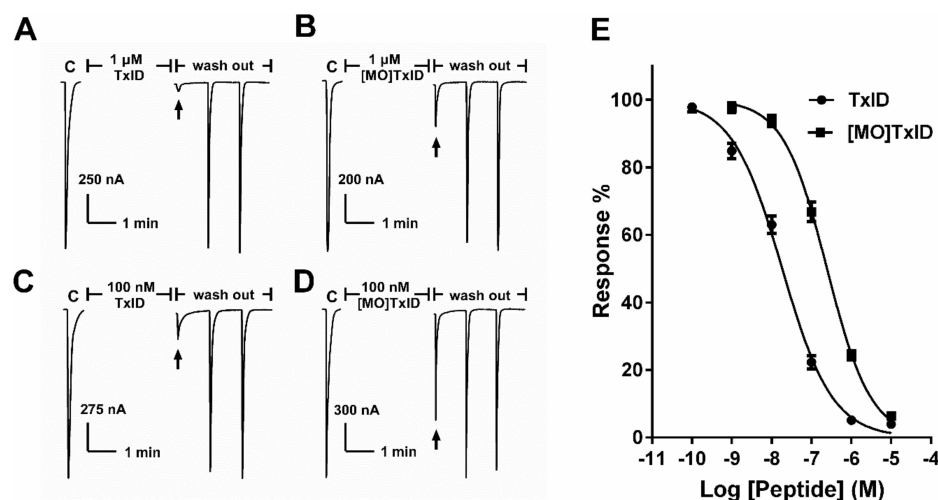


Figure 3. $\alpha 3\beta 4$ nAChR-inhibitory activities of TxID and [MO]TxID. $\alpha 3\beta 4$ nAChR was expressed in *Xenopus* oocytes as described under “Materials and Methods.” (A) TxID at 1 μ M was added to the chamber and incubated with oocyte for 5 min. Then TxID was washed out and the response to 1-s pulses to ACh was again measured (arrow). “C” indicates control responses to ACh; (B) Representative ACh-evoked currents of rat $\alpha 3\beta 4$ nAChR obtained in presence of [MO]TxID at 1 μ M; (C) Representative ACh-evoked currents of rat $\alpha 3\beta 4$ nAChR obtained that the oocyte was exposed to 100 nM TxID; (D) a representative response of one typical oocyte was exposed to 100 nM [MO]TxID; (E) Concentration-response analysis of the activities of TxID and [MO]TxID on rat $\alpha 3\beta 4$ nAChR subtype. Error bars denote the means \pm SEM. of the data from 3 to 8 separate oocytes.

Table 1. IC₅₀ and Hill slope values for blockade of $\alpha 3\beta 4$ nAChR subtype by TxID analogues.

TxID Analogues	$\alpha 3\beta 4$ nAChR, IC ₅₀ *	Hill Slope *	IC ₅₀ Ratio Relative to TxID
TxID	18.38 (15.35–22.0)	0.69 (0.61–0.77)	1
[MO]TxID	245.0 (211.7–283.6)	0.79 (0.71–0.87)	13.3
[M11V]TxID	980.3 (760.1–1264)	0.88 (0.68–1.09)	53.3
[M11I]TxID	69.09 (50.68–94.19)	0.70 (0.57–0.83)	3.8
[M11L]TxID	256.7 (211.7–311.2)	1.27 (1.01–1.54)	14.0
[M11K]TxID	>10,000 ^a	-	-
[M11R]TxID	>10,000 ^a	-	-
[M11Q]TxID	>10,000 ^a	-	-
[M11E]TxID	>10,000 ^a	-	-
[M11A]TxID	>10,000 ^a	-	-

* Numbers in parentheses are 95% confidence intervals. ^a Less than 50% block at 10 μ M.

2.3. Effect of Mutants of Substitution at Met of TxID on $\alpha 3\beta 4$ nAChR Subtype

The methionine of TxID was substituted by Ala, hydrophobic amino acids (Ile, Val and Leu) and charged amino acid (Lys, Arg, Glu and Gln) and these analogues (1 μ M) were tested at $\alpha 3\beta 4$ nAChR (Figure 4A). The [M11K]TxID, [M11R]TxID, [M11Q]TxID, [M11A]TxID and [M11E]TxID exhibited nearly no inhibition on $\alpha 3\beta 4$ nAChR. Replacing the Met residue with Val resulted in a 40% decrease on blocking $\alpha 3\beta 4$ nAChR. In contrast, [M11I]TxID and [M11L]TxID displayed comparable activity to the native peptide, which blocked >80% evoked current (Figure 4A).

The concentration-response relationships of all TxID analogues were determined (Figure 4B, Table 1). Three of them retained the potency on $\alpha 3\beta 4$ subtype, and none of the analogues increased binding affinity compared to native peptide. The IC₅₀ for [M11I]TxID on $\alpha 3\beta 4$ nAChR subtype was 69.09 nM, which retained comparable activity compared to native peptide. Surprisingly, the activities of [M11L]TxID and [M11V]TxID reduced dramatically with an IC₅₀ of 256.7 nM and 980.3 nM respectively (Table 1). There were 14-fold potency loss for [M11L]TxID and 53-fold potency loss for [M11V]TxID.

We subsequently evaluated [M11L]TxID and [M11I]TxID on the other nAChR subtypes, including $\alpha 6/\alpha 3\beta 4$, $M\alpha 1\beta 1\delta\epsilon$, $\alpha 7$, $\alpha 9\alpha 10$, $\alpha 2\beta 4$, $\alpha 3\beta 2$, $\alpha 4\beta 2$ and $\alpha 4\beta 4$. Only $\alpha 6/\alpha 3\beta 4$ nAChR can be blocked with high concentration of 10 μM .

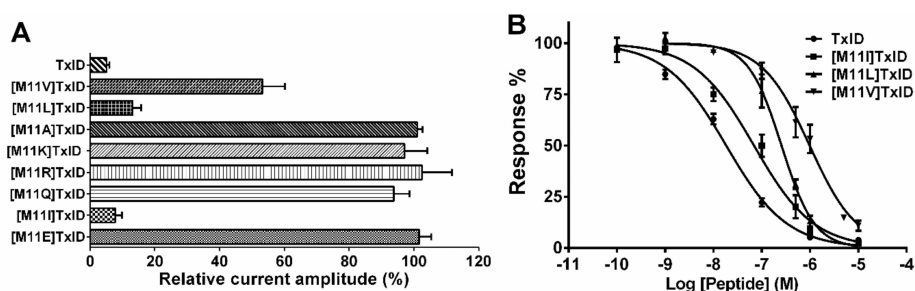


Figure 4. Inhibition of $\alpha 3\beta 4$ nAChR by TxID and its Met substitution analogues. (A) Bar graph of normalized inhibition of ACh-evoked current is generated by methionine-substituted TxID analogues and native TxID. All peptides were tested at 1 μM and data are represented as mean \pm SEM ($n = 3-6$); (B) Concentration-response curves are obtained for inhibition of $\alpha 3\beta 4$ nAChR. Error bars denote the means \pm SEM of the data from 3 to 8 separate oocytes.

2.4. Homology Modeling and MD Simulations Demonstrate Potency Variation between TxID Analogues and $\alpha 3\beta 4$ nAChR

Homology modeling/MD simulations were performed to understand the molecular mechanism for the activity of TxID analogues at $\alpha 3\beta 4$ nAChR. Native TxID and its mutants bind to the extracellular domain of the rat $\alpha 3\beta 4$ nAChR and the models demonstrate the binding pocket of peptides complexed with $\alpha 3\beta 4$ nAChR (Figure 5). According to the model, Met-11 is surrounded by hydrophobic and charged amino acids in $\beta 4$ subunit, including Ile78, Ile110, Arg112 and Arg80 (Figure 5A). Therefore, the substitution of Met by charged amino acids ([M11K]TxID, [M11R]TxID and [M11Q]TxID) would significantly impact the electrostatic interactions between peptides and receptors, which may result in a complete loss of inhibition at $\alpha 3\beta 4$ nAChR. Through 50 ns dynamic stimulation, the distance between MetO and $\beta 4$ subunit increases and MetO is impacted by more amino acids in $\alpha 3$ subunit, including Ser149, Tyr150 and Asp154 (Figure 5B). In addition, [MO]TxID is more hydrophilic than wildtype toxin, hence MetO would probably decrease hydrophobic interactions with Ile78 and Ile110. Besides, when Met residue was mutated to Ile residue, distance between two hydrophobic surfaces also increases, which partially weakens the interaction force of Ile-11 and receptors. Similarly, replacement of Met with Leu and Val leads to lose more potency on $\alpha 3\beta 4$ nAChR.

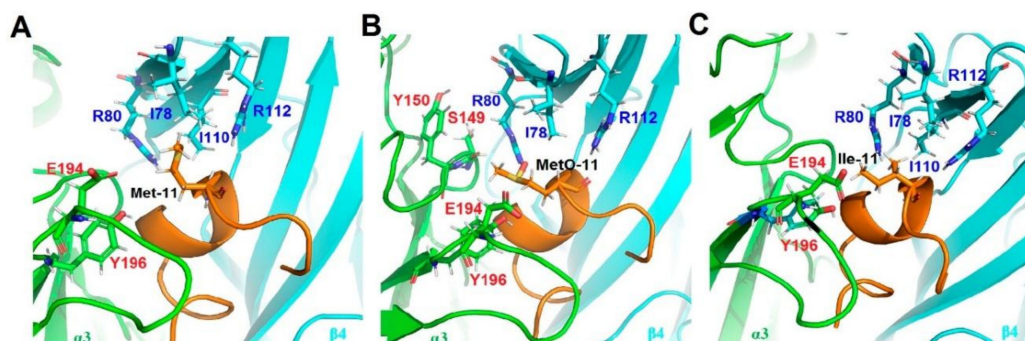


Figure 5. Molecular interactions between peptides and $\alpha 3\beta 4$ nAChR through homology modeling and MD simulation. The $\alpha 3$ subunit is drawn in green, the $\beta 4$ is in cyan, and the peptides are in brown. Amino acids around 4 \AA radius of the Met and its substitutions are labeled. (A) The molecular model was shown between TxID and $\alpha 3\beta 4$ nAChR during 50 ns MD simulations; (B) Snapshot at 50 ns of [MO]TxID and $\alpha 3\beta 4$ interface; (C) Snapshot at 50 ns of [M11I]TxID and $\alpha 3\beta 4$ interface.

3. Discussion

Cone snails have evolved many conopeptides which target to a wide variety of different voltage- or ligand-gated ion channels. The α -family conotoxins (α^* -CTxs) act by blocking different isoforms of nAChRs, which locate in the neuromuscular junction or central nervous system broadly [5,6]. Methionine, sulfur-containing amino acid, was exist in different conotoxin families, such as α -, α D-, α O- and ω -CTxs (Table 2) [11,15–28]. Apart from TxID, several α -CTxs contain Met residue. SrIA and SrIB were discovered from the venom of *Conus spurius*, which can inhibit $\alpha 4\beta 2$ and $\alpha 1\beta 1\gamma\delta$ nAChR, respectively [15]. EI demonstrates strong blockade of the nAChR subtypes of $\alpha 4\beta 2$, $\alpha 1\beta 1\gamma\delta$ and $\alpha 3\beta 4$ [15,16]. Additionally, methionine was detected in several α D-CTxs which formed dimer and bound different nAChR subtypes [25,26]. The ω -CTx MVIIA is a potent antagonist of N-type calcium ion channel (Cav2.2), which is the only cone snail-derived pharmaceutical drug. MVIIA contains a Met at the 12th position. Before it was developed as a drug candidate, hundreds of analogues of wild type peptide were tested. However, there was no ideal analogue substituting MVIIA, which indicated the difficulty to reform native peptide [29]. Pu14a containing Met at position 10 inhibits neuronal $\alpha 3\beta 2$ and neuromuscular $\alpha 1\beta 1\gamma\delta$ nAChR [27]. Recently, a novel O-superfamily conotoxin, α O-GeXXVIIA, a disulfide-linked homodimer conopeptide, blocks $\alpha 9\alpha 10$ nAChR with high potency [28]. Therefore, the methionine possibly plays an important role in the modulation of the interaction between conotoxins and receptors.

Table 2. Sequences and receptor activities of conotoxins comprising Met residue. #, amidated C-terminus; γ , γ -carboxyglutamate; O, 4-trans-hydroxyproline; Z, pyroglutamate. The Met residues are in bold.

Peptide	Species	Sequence	Activities	Reference
α -TxID	<i>C. textile</i>	GCCSHPVCSAMSPIC#	$\alpha 3\beta 4 > \alpha 6 / \alpha 3\beta 4 > \alpha 2\beta 4$	[11]
α -SrIA	<i>C. spurius</i>	RTCCSROTCRM γ YP γ LCG#	$\alpha 1\beta 1\gamma\delta$, $\alpha 4\beta 2$	[15]
α -SrIB	<i>C. spurius</i>	RTCCSROTCRM γ YP γ LCG#	$\alpha 1\beta 1\gamma\delta$, $\alpha 4\beta 2$	[15]
α -EI	<i>C. ermineus</i>	RDOCCYHPTCNMSNPQIC#	$\alpha 1\beta 1\gamma\delta$, $\alpha 3\beta 4$, $\alpha 4\beta 2$	[15,16]
ω -CnVIIA	<i>C. consors</i>	CKGKGAOCTRLMYDCCHGSCSSSKGRC#	$Ca_{2.2} > Ca_{2.1}$	[17]
ω -CVIB	<i>C. catus</i>	KGKGASCRKTM γ DCCRGSCRSRGRC#	$Ca_{2.2} \sim Ca_{2.1} > Ca_{2.3}$	[18]
ω -CVIC	<i>C. catus</i>	CKGKGQSCSKL γ MYDCCTGSCSRRGK#	$Ca_{2.1} \sim Ca_{2.2}$	[18]
ω -CVID	<i>C. catus</i>	CKSKGAKCSKLM γ DCCSGSCSGTVGRC#	$Ca_{2.2} > Ca_{2.1}$	[18]
ω -MVIIA	<i>C. magus</i>	CKGKGAKCSRLMYDCCTGSCRSRGK#	$Ca_{2.2} > Ca_{2.1}$	[19–21]
ω -MVIIC	<i>C. magus</i>	CKGKGAPCSKTM γ DCCSGSCGRRGK#	$Ca_{2.1} > Ca_{2.2}$	[21,22]
ω -MVIID	<i>C. magus</i>	CQGRGASCRKTM γ NCCSGSCNRGRCC#	$Ca_{2.1} \gg Ca_{2.2}$	[23,24]
α D-V \times XXA	<i>C. vexillum</i>	DVQDCQVSTOGSKWGRCCLN γ RVCGPM CCPASHCYCVYHRGRGHGCS (dimer)	N.D.	[25]
α D-V \times XXB	<i>C. vexillum</i>	DD γ S γ CIINTRDSPWGRCCRTMCGSMCC PRNGCTCVYHWRRGHGCS (dimer)	$\alpha 7$, $\alpha 3\beta 2$, $\alpha 4\beta 2$	[25]
α D-V \times XXC	<i>C. vexillum</i>	DLRQCTR γ NAPGSTWGRCCLN γ PMCGNFC CPRSGCTCAYNRRGIYCS (dimer)	N.D.	[25]
α D-cap	<i>C. capitaneus</i>	EVQECQVDTPGSSWGKCCMTRMCGTMC CSRSVCTCVYHWRRGHGCS (dimer)	$\alpha 7$, $\alpha 3\beta 2$, $\alpha 4\beta 2$	[26]
α D-mus	<i>C. mustelinus</i>	DVRECQVNTPGSKWGKCCMTRMCGTMC CARSGCTCVYHWRRGHGCS (dimer)	$\alpha 7$, $\alpha 3\beta 2$, $\alpha 4\beta 2$	[26]
Pu14a	<i>C. pulicarius</i>	DCPPHPVPGMHKCVCLKTC	$\alpha 3\beta 2$, $\alpha 6\alpha 3\beta 2$	[27]
O-GeXXVIIA	<i>C. generalis</i>	ALMSTGTNYRLLKTCRGSGRYCRSPYDCR RRCRRISDACV	$\alpha 9\alpha 10$, $\alpha 1\beta 1\epsilon\delta$	[28]

Increasing evidences indicate that Met residue in proteins is the same as cysteine which serve as antioxidants and impact the structure of proteins [14]. Here, we investigated how methionine

played a role in interaction between TxID and $\alpha 3\beta 4$ nAChR. Firstly, [MO]TxID was synthesized and the potency on $\alpha 3\beta 4$ nAChR was tested. It resulted in a 13.3-fold loss of activity compared to parent peptide. Previous study showed single amino acid substitutions in TxID shifted its selectivity. Analogously, Met oxidation in TxID probably change its specificity on $\alpha 3\beta 4$ nAChR. To understand the role of Met in TxID, we systematically substituted Met residue by the other eight amino acids, including Ala, Ile, Val, Leu, Lys, Arg, Glu and Gln. Most analogues decreased or even lost the affinity at $\alpha 3\beta 4$ nAChR. Only [M11I]TxID retained most activity on $\alpha 3\beta 4$ nAChR (Table 1). Our findings show that [M11L]TxID binds with Hill coefficient of 1.27 and other TxID analogues bind with Hill coefficients less than 1 (0.69–0.88), which may predict the substitution of Met in TxID can allosterically regulate the conformation of $\alpha 3\beta 4$ nAChR [30]. Consistent with the electrophysiology experiment results, the MD simulations data shows that Met residue can establish hydrophobic interactions with the residues in the binding pocket. In our models, the conversion of Met to MetO weakens the hydrophobic interaction between peptide and receptor. It is, therefore, not surprising to find the [MO]TxID have a decreased activity compared to TxID. Eight analogues were designed and synthesized. Their potencies were evaluated respectively to reveal effects of the 11th position amino acid of TxID on $\alpha 3\beta 4$ nAChR. Among them, replacement of Met with Ile is only 3.8-fold less active against $\alpha 3\beta 4$ nAChR. In the binding mode of [M11I]TxID at $\alpha 3\beta 4$ nAChR, the spacing distance between position 11 and $\beta 4$ (-)I78 increased from 3.5 Å to 4.6 Å, which may slightly but not significantly weaken the hydrophobic interaction, which could be used to explain why [M11I]TxID has comparable activity relative to the parent peptide (Figure 6).

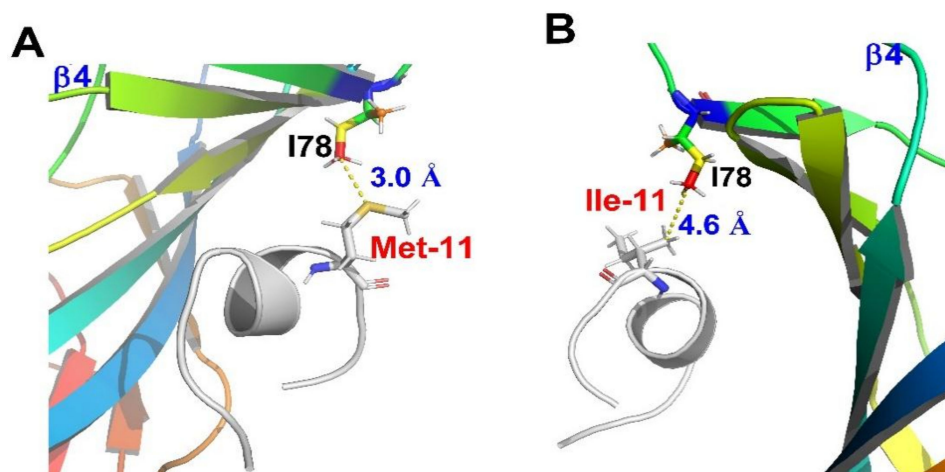


Figure 6. MD simulations demonstrate the distance difference between rat $\beta 4$ -I78 and Met-11 or Ile-11. (A) For native TxID, the distance between the sulfur atom of Met-11 and side-chain C δ of $\beta 4$ -I78 lies within 3.5 Å; (B) For analogue [M11I]TxID, the distance between C $\gamma 2$ of Ile-11 and side-chain C δ of $\beta 4$ -I78 is 4.6 Å.

To date, several α -CTxs and its analogues have been identified to antagonize $\alpha 3\beta 4$ nAChR [11,31–34]. $\alpha 4/6$ -CTx AuIB, from the venom of *Conus aulicus*, selectively inhibits $\alpha 3\beta 4$ nAChR with an IC₅₀ of 750 nM [31]. Alanine-scanning and MD simulations analysis revealed the side chain size, aromaticity, and hydrophobicity of phenylalanine (Phe) at position 9 can significantly affect the activity of AuIB at $\alpha 3\beta 4$ nAChR [35]. α -CTx RegIIA was identified from *Conus regius* venom, inhibiting $\alpha 3\beta 2$, $\alpha 3\beta 4$, and $\alpha 7$ nAChRs [34]. Mutagenesis of RegIIA revealed α -CTx [N11A, N12A] RegIIA specific blocked $\alpha 3\beta 4$ nAChR, then the molecular mechanism research suggested Asn-9, Asn-11, and Asn-12 involved in toxin-receptor interaction [36]. Another research elucidated specific β subunit residues interacting with RegIIA and AuIB [37]. Combining with our research results, the interaction between α -CTxs with $\alpha 3\beta 4$ nAChR is complex, and further mutational and molecular mechanical studies are required to illuminate SAR between them.

Owing to its potent activity, the TxID has a potential in the development of a novel drug. Unfortunately, the conversion of Met to MetO is readily to happen during TxID synthesis and oxidation steps as well as under oxidative environment in vivo, which causes the loss of activity in the inhibition of $\alpha 3\beta 4$ nAChR. Furthermore, conotoxins containing Met require low-temperature storage in the entire supply chain which increases the inconvenience and cost [38]. These drawbacks caused by Met should be considered in the pharmaceutical industry when transferring TxID to a drug. Hence, it is an ideal strategy that Met could be replaced by other stable amino acids or derivatives while maintaining its original activity. In this study, our research results showed substitution Met-11 with Ile retained comparable activity at $\alpha 3\beta 4$ nAChR. Our research sheds a light on re-engineering conotoxins containing Met to retain their stability and activity.

In summary, we firstly investigated how the conversion of Met to MetO affected the efficacy of TxID at the $\alpha 3\beta 4$ nAChR. The substitution of Met of TxID by an Ile maintained the comparable activity at the $\alpha 3\beta 4$ nAChR. Homology models and dynamic simulation suggested the molecular mechanism of interaction between different analogues of TxID and $\alpha 3\beta 4$ nAChR. These findings provide further information for understanding the function of Met residue in α -CTx TxID.

4. Materials and Methods

4.1. Chemical Synthesis and Oxidative Folding of α -Ctx TxID Analogues

The linear peptides of TxID and its mutants were synthesized as previously described [39]. Two disulfide bonds between cysteine residues form disulfide frameworks with regioselective protection method. Cysteine residues were protected with a pairwise combination of S-trityl on Cys I and Cys III and with S-acetamidomethyl on Cys II and IV. Acid-labile protecting groups Trt were cleaved from Cys I and Cys III during the acidic conditions, and the first disulfide bridge was formed by exposure to potassium ferricyanide ($\text{K}_3[\text{Fe}(\text{CN})_6]$), then monocyclic peptides were purified by preparative RP-HPLC. The Acn protecting groups were subsequently removed and closed from Cys II and Cys IV by iodine oxidation. The synthesized peptides were purified on a Waters 2535 HPLC system (Milford, MA, USA) using preparative Vydac C18 column with a linear gradient of a 10–40% eluate B, and 90–60% eluate a over 30 min. Solvent B was 90% ACN, 0.092% TFA, and H_2O ; Solvent a was 0.1% TFA in H_2O . The purity of the TxID and its analogues were determined by monitoring absorbance at 214 nm during HPLC ($\geq 95\%$ purity). ESI-MS mass spectrometry was utilized to confirm the identity of the products.

4.2. Chemical Synthesis of [MO]TxID

Met is easily modified to methionine sulfoxide under oxidative conditions. α -Ctx TxID (0.2 mg) firstly dissolved in 100 μL of 60% acetonitrile in ddH_2O , which was incubated with 5 mL of 10% hydrogen peroxide (H_2O_2) in 20 min at room temperature. Then reaction products were separated using semi-preparative RP-HPLC with a linear gradient as above conditions. The purity of oxidative products was identified by Waters ACQUITY UPLC™ System with BEH300 C18 column (50×2.1 mm, 1.7 μm) (Waters Corporation, Milford, MA, USA). The molecular mass was measured on a Waters TQD mass spectrometer equipped with an electrospray ionization source (Waters Corporation, Milford, MA, USA).

4.3. RNA Preparation and Injection

Plasmid DNAs encoding rat nAChR subunits were kindly provided by Stefan H. Heinemann (Salk Institute, San Diego, CA, USA). The plasmids were linearized with appropriate restriction enzymes. Then capped RNA (cRNA) for the various subunits were made using transcription kit of the mMessage mMachine SP6 (Ambion, Austin, TX, USA) in vitro. The cRNA was purified using MEGAclear™ kit (Ambion). The concentration of each cRNA was determined using Smart Spec™ plus Spectrophotometer (Bio-Rad, Hercules, CA, USA) at 260 nm. cRNA of the various subunits was combined to give ~ 50 ng/ μL of each subunit cRNA. 50.6 nL of this mixture was injected into

each *Xenopus* oocyte with a Drummond microdispenser (Drummond Scientific, Broomall, PA, USA), and incubated at 17 °C. Oocytes were injected within 1 day of harvesting, and recordings were made 2–4 days post-injection.

4.4. Voltage-Clamp Recording

Oocytes were voltage-clamped and exposed to ACh and CTxs as described previously [40]. Briefly, oocytes were transferred into the recording chamber (~50 µL in volume) and gravity-perfused at 2 mL/min with ND96 buffer (96 mM NaCl, 2.0 mM KCl, 1.0 mM MgCl₂·6H₂O, 1.8 mM CaCl₂·2H₂O, 5 mM HEPES, pH 7.1–7.5) containing 1 µM atropine and 0.1 mg/mL bovine serum albumin (BSA). For α9α10 subtype, the ND96 contained no atropine. Two electrode voltage clamp recordings from oocytes were carried out at room temperature using an Axoclamp 900A amplifier (Molecular Devices Corp., Sunnyvale, CA, USA) at a holding potential of −70 mV. The continuous gravity perfused with standard ND96 solution and stimulated with 1-s pulses of ACh once every minute. For screening of receptor for toxin concentration 10 µM and lower, once a stable baseline was achieved, we added 5 µL of different concentration toxin to the chamber and waited for 5 min, then applied perfusion system, during which 1-s pulses of 100 µM ACh were applied every minute until a constant level of block was achieved. The electrophysiology data were recorded and analyzed using Clampfit 10.2 software (Molecular Devices Corp., Sunnyvale, CA, USA). The results were acquired with at least three oocytes.

4.5. Statistical Analysis of Data

The data and statistical analysis in this study comply with previous strategy [12]. An average of five control responses just preceding a test response was used to normalize the test response to obtain “% response”. All electrophysiological data were collected at least three oocytes and represent means ± standard error of the mean (SEM). The dose-response data were fit to the equation, % response = 100 / {1 + ([toxin]/IC₅₀)^{n_H}}, where n_H is the Hill coefficient, by nonlinear regression analysis using GraphPad Prism 5.0 (GraphPad Software, San Diego, CA, USA).

4.6. Homology Modeling

Homology models of the extracellular ligand binding domain of Rat α3β4 nAChR were generated using Modeler9v14 as previous method [13,41]. The co-crystal structure of Ac-AChBP (*Aplysia californica* acetylcholine-binding protein) with the potent mutant TxIA(A10L) (PDB ID: 2BR8) [42] and crystallographic structure of human α9 subunit (PDB ID: 4D01) [43] were adopted as structural template. These templates were chosen to generate model of the interaction between toxin and rat α3β4 nAChR ligand binding domains. Then the model was selected for subsequent molecular dynamics (MD) simulations and analysis.

4.7. Molecular Dynamics Simulations

Molecular dynamics (MD) simulations were performed for the α3β4 nAChRs with TxID and its two analogues. The structure of methionine sulfoxide was built with GaussView V.5 and Amber tools 14. These models were implemented using the GROMACS5.1 [44] with the amber ff99SB-ILDN30 force field [45]. The MD parameters complied with previous study. 50 nanoseconds simulation was performed for each model and graphics were produced using PyMOL package (<http://www.pymol.org/>).

Author Contributions: J.R., Y.W., and S.L. conceived and designed the experiments; J.R., Y.W., R.L. and J.N. performed the experiments; J.R., X.Z., D.Z. and S.L. analyzed the data; J.R., Y.W. and S.L. wrote the paper.

Acknowledgments: This work was supported by National Natural Science Foundation of China (No. 81660585, No. 31760249), Major International Joint Research Project of National Natural Science Foundation of China (81420108028), Hainan University Youth foundation (hdkyx201725), Changjiang Scholars and Innovative Research Team in University Grant (IRT_15R15).

Conflicts of Interest: The authors declare no conflict of interest.

References

1. Lewis, R.J.; Dutertre, S.; Vetter, I.; Christie, M.J. Conus venom peptide pharmacology. *Pharmacol. Rev.* **2012**, *64*, 259–298. [[CrossRef](#)] [[PubMed](#)]
2. Terlau, H.; Olivera, B.M. Conus venoms: a rich source of novel ion channel-targeted peptides. *Physiol. Rev.* **2004**, *84*, 41–68. [[CrossRef](#)] [[PubMed](#)]
3. Robinson, S.D.; Norton, R.S. Conotoxin gene superfamilies. *Mar. Drugs* **2014**, *12*, 6058–6101. [[CrossRef](#)] [[PubMed](#)]
4. Essack, M.; Bajic, V.B.; Archer, J.A. Conotoxins that confer therapeutic possibilities. *Mar. Drugs* **2012**, *10*, 1244–1265. [[CrossRef](#)] [[PubMed](#)]
5. Azam, L.; McIntosh, J.M. Alpha-conotoxins as pharmacological probes of nicotinic acetylcholine receptors. *Acta Pharmacol. Sin.* **2009**, *30*, 771–783. [[CrossRef](#)] [[PubMed](#)]
6. Akondi, K.B.; Muttenthaler, M.; Dutertre, S.; Kaas, Q.; Craik, D.J.; Lewis, R.J.; Alewood, P.F. Discovery, synthesis, and structure-activity relationships of conotoxins. *Chem. Rev.* **2014**, *114*, 5815–5847. [[CrossRef](#)] [[PubMed](#)]
7. Muttenthaler, M.; Akondi, K.B.; Alewood, P.F. Structure-activity studies on alpha-conotoxins. *Curr. Pharm. Des.* **2011**, *17*, 4226–4241. [[CrossRef](#)] [[PubMed](#)]
8. McIntosh, J.M.; Santos, A.D.; Olivera, B.M. Conus peptides targeted to specific nicotinic acetylcholine receptor subtypes. *Annu. Rev. Biochem.* **1999**, *68*, 59–88. [[CrossRef](#)] [[PubMed](#)]
9. Hurst, R.; Rollema, H.; Bertrand, D. Nicotinic acetylcholine receptors: From basic science to therapeutics. *Pharmacol. Ther.* **2013**, *137*, 22–54. [[CrossRef](#)] [[PubMed](#)]
10. Albuquerque, E.X.; Pereira, E.F.; Alkondon, M.; Rogers, S.W. Mammalian nicotinic acetylcholine receptors: From structure to function. *Physiol. Rev.* **2009**, *89*, 73–120. [[CrossRef](#)] [[PubMed](#)]
11. Luo, S.; Zhangsun, D.; Zhu, X.; Wu, Y.; Hu, Y.; Christensen, S.; Harvey, P.J.; Akcan, M.; Craik, D.J.; McIntosh, J.M. Characterization of a novel alpha-conotoxin TxID from *Conus textile* that potently blocks rat alpha3beta4 nicotinic acetylcholine receptors. *J. Med. Chem.* **2013**, *56*, 9655–9663. [[CrossRef](#)] [[PubMed](#)]
12. Zhangsun, D.; Wu, Y.; Zhu, X.; Luo, S. Sensitivity of α -Conotoxin TxID on stoichiometry of α 3 β 4 nicotinic acetylcholine receptors. *Chin. Pharm. J.* **2016**, *51*, 802–808.
13. Wu, Y.; Zhangsun, D.; Zhu, X.; Kaas, Q.; Zhangsun, M.; Harvey, P.J.; Craik, D.J.; McIntosh, J.M.; Luo, S. Alpha-conotoxin [S9A]TxID potently discriminates between alpha3beta4 and alpha6/alpha3beta4 nicotinic acetylcholine receptors. *J. Med. Chem.* **2017**, *60*, 5826–5833. [[CrossRef](#)] [[PubMed](#)]
14. Kim, G.; Weiss, S.J.; Levine, R.L. Methionine oxidation and reduction in proteins. *Biochim. Biophys. Acta* **2014**, *1840*, 901–905. [[CrossRef](#)] [[PubMed](#)]
15. Lopez-Vera, E.; Aguilar, M.B.; Schiavon, E.; Marinzi, C.; Ortiz, E.; Restano Cassulini, R.; Batista, C.V.; Possani, L.D.; Heimer de la Cotera, E.P.; Peri, F.; et al. Novel alpha-conotoxins from *Conus spurius* and the alpha-conotoxin EI share high-affinity potentiation and low-affinity inhibition of nicotinic acetylcholine receptors. *FEBS J.* **2007**, *274*, 3972–3985. [[CrossRef](#)] [[PubMed](#)]
16. Martinez, J.S.; Olivera, B.M.; Gray, W.R.; Craig, A.G.; Groebe, D.R.; Abramson, S.N.; McIntosh, J.M. Alpha-conotoxin EI, a new nicotinic acetylcholine receptor antagonist with novel selectivity. *Biochemistry* **1995**, *34*, 14519–14526. [[CrossRef](#)] [[PubMed](#)]
17. Favreau, P.; Gilles, N.; Lamthanh, H.; Bournaud, R.; Shimahara, T.; Bouet, F.; Laboute, P.; Letourneux, Y.; Menez, A.; Molgo, J.; et al. a new omega-conotoxin that targets n-type voltage-sensitive calcium channels with unusual specificity. *Biochemistry* **2001**, *40*, 14567–14575. [[CrossRef](#)] [[PubMed](#)]
18. Lewis, R.J.; Nielsen, K.J.; Craik, D.J.; Loughnan, M.L.; Adams, D.A.; Sharpe, I.A.; Luchian, T.; Adams, D.J.; Bond, T.; Thomas, L.; et al. Novel omega-conotoxins from *Conus catus* discriminate among neuronal calcium channel subtypes. *J. Biol. Chem.* **2000**, *275*, 35335–35344. [[CrossRef](#)] [[PubMed](#)]
19. Olivera, B.M.; Cruz, L.J.; de Santos, V.; LeCheminant, G.W.; Griffin, D.; Zeikus, R.; McIntosh, J.M.; Galyean, R.; Varga, J.; Gray, W.R.; et al. Neuronal calcium channel antagonists. Discrimination between calcium channel subtypes using omega-conotoxin from *Conus magus* venom. *Biochemistry* **1987**, *26*, 2086–2090. [[CrossRef](#)] [[PubMed](#)]
20. Kim, J.I.; Takahashi, M.; Ohtake, A.; Wakamiya, A.; Sato, K. Tyr13 is essential for the activity of omega-conotoxin MVIIA and GVIA, specific n-type calcium channel blockers. *Biochem. Biophys. Res. Commun.* **1995**, *206*, 449–454. [[CrossRef](#)] [[PubMed](#)]

21. Nielsen, K.J.; Adams, D.; Thomas, L.; Bond, T.; Alewood, P.F.; Craik, D.J.; Lewis, R.J. Structure-activity relationships of omega-conotoxins mviiia, mviiic and 14 loop splice hybrids at n and p/q-type calcium channels. *J. Mol. Biol.* **1999**, *289*, 1405–1421. [[CrossRef](#)] [[PubMed](#)]
22. Hillyard, D.R.; Monje, V.D.; Mintz, I.M.; Bean, B.P.; Nadasdi, L.; Ramachandran, J.; Miljanich, G.; Azimi-Zoonooz, A.; McIntosh, J.M.; Cruz, L.J.; et al. a new conus peptide ligand for mammalian presynaptic Ca²⁺ channels. *Neuron* **1992**, *9*, 69–77. [[CrossRef](#)]
23. Haack, J.A.; Kinser, P.; Yoshikami, D.; Olivera, B.M. Biotinylated derivatives of omega-conotoxins gvia and mviid: Probes for neuronal calcium channels. *Neuropharmacology* **1993**, *32*, 1151–1159. [[CrossRef](#)]
24. Monje, V.D.; Haack, J.A.; Naisbitt, S.R.; Miljanich, G.; Ramachandran, J.; Nadasdi, L.; Olivera, B.M.; Hillyard, D.R.; Gray, W.R. a new conus peptide ligand for ca channel subtypes. *Neuropharmacology* **1993**, *32*, 1141–1149. [[CrossRef](#)]
25. Loughnan, M.; Nicke, A.; Jones, A.; Schroeder, C.I.; Nevin, S.T.; Adams, D.J.; Alewood, P.F.; Lewis, R.J. Identification of a novel class of nicotinic receptor antagonists: Dimeric conotoxins vxxiia, vxxiib, and vxxiic from *Conus vexillum*. *J. Biol. Chem.* **2006**, *281*, 24745–24755. [[CrossRef](#)] [[PubMed](#)]
26. Kaufenstein, S.; Kendel, Y.; Nicke, A.; Coronas, F.I.; Possani, L.D.; Favreau, P.; Krizaj, I.; Wunder, C.; Kauert, G.; Mebs, D. New conopeptides of the d-superfamily selectively inhibiting neuronal nicotinic acetylcholine receptors. *Toxicon* **2009**, *54*, 295–301. [[CrossRef](#)] [[PubMed](#)]
27. Peng, C.; Ye, M.; Wang, Y.; Shao, X.; Yuan, D.; Liu, J.; Hawrot, E.; Wang, C.; Chi, C. a new subfamily of conotoxins belonging to the a-superfamily. *Peptides* **2010**, *31*, 2009–2016. [[CrossRef](#)] [[PubMed](#)]
28. Jiang, S.; Tae, H.S.; Xu, S.; Shao, X.; Adams, D.J.; Wang, C. Identification of a novel O-conotoxin reveals an unusual and potent inhibitor of the human alpha9alpha10 nicotinic acetylcholine receptor. *Mar. Drugs* **2017**, *15*, 170. [[CrossRef](#)] [[PubMed](#)]
29. Miljanich, G.P. Ziconotide: Neuronal calcium channel blocker for treating severe chronic pain. *Curr. Med. Chem.* **2004**, *11*, 3029–3040. [[CrossRef](#)] [[PubMed](#)]
30. Heino, P. Hill coefficients, dose-response curves and allosteric mechanisms. *J. Chem. Biol.* **2010**, *3*, 37–44.
31. Luo, S.Q.; Kulak, J.M.; Cartier, G.E.; Jacobsen, R.B.; Yoshikami, D.; Olivera, B.M.; McIntosh, J.M. Alpha-conotoxin AulB selectively blocks alpha3 beta4 nicotinic acetylcholine receptors and nicotine-evoked norepinephrine release. *J. Neurosci.* **1998**, *18*, 8571–8579. [[CrossRef](#)] [[PubMed](#)]
32. Azam, L.; Dowell, C.; Watkins, M.; Stitzel, J.A.; Olivera, B.M.; McIntosh, J.M. Alpha-conotoxin BuIA, a novel peptide from *Conus bullatus*, distinguishes among neuronal nicotinic acetylcholine receptors. *J. Biol. Chem.* **2005**, *280*, 80–87. [[CrossRef](#)] [[PubMed](#)]
33. McIntosh, J.M.; Plazas, P.V.; Watkins, M.; Gomez-Casati, M.E.; Olivera, B.M.; Elgoyhen, A.B. a novel alpha-conotoxin, PeIA, cloned from *Conus pergrandis*, discriminates between rat alpha9alpha10 and alpha7 nicotinic cholinergic receptors. *J. Biol. Chem.* **2005**, *280*, 30107–30112. [[CrossRef](#)] [[PubMed](#)]
34. Franco, A.; Kompella, S.N.; Akondi, K.B.; Melaun, C.; Daly, N.L.; Luetje, C.W.; Alewood, P.F.; Craik, D.J.; Adams, D.J.; Mari, F. RegIIA: An alpha4/7-conotoxin from the venom of *Conus regius* that potently blocks alpha3beta4 nachrs. *Biochem. Pharmacol.* **2012**, *83*, 419–426. [[CrossRef](#)] [[PubMed](#)]
35. Grishin, A.A.; Cuny, H.; Hung, A.; Clark, R.J.; Brust, A.; Akondi, K.; Alewood, P.F.; Craik, D.J.; Adams, D.J. Identifying key amino acid residues that affect alpha-conotoxin AulB inhibition of alpha3beta4 nicotinic acetylcholine receptors. *J. Biol. Chem.* **2013**, *288*, 34428–34442. [[CrossRef](#)] [[PubMed](#)]
36. Kompella, S.N.; Hung, A.; Clark, R.J.; Mari, F.; Adams, D.J. Alanine scan of alpha-conotoxin RegIIA reveals a selective alpha3beta4 nicotinic acetylcholine receptor antagonist. *J. Biol. Chem.* **2015**, *290*, 1039–1048. [[CrossRef](#)] [[PubMed](#)]
37. Cuny, H.; Kompella, S.N.; Tae, H.S.; Yu, R.; Adams, D.J. Key structural determinants in the agonist binding loops of human beta2 and beta4 nicotinic acetylcholine receptor subunits contribute to alpha3beta4 subtype selectivity of alpha-conotoxins. *J. Biol. Chem.* **2016**, *291*, 23779–23792. [[CrossRef](#)] [[PubMed](#)]
38. Craik, D.J.; Adams, D.J. Chemical modification of conotoxins to improve stability and activity. *ACS Chem. Biol.* **2007**, *2*, 457–468. [[CrossRef](#)] [[PubMed](#)]
39. Luo, S.; Akondi, K.B.; Zhangsun, D.; Wu, Y.; Zhu, X.; Hu, Y.; Christensen, S.; Dowell, C.; Daly, N.L.; Craik, D.J.; et al. Atypical alpha-conotoxin LtIA from *Conus litteratus* targets a novel microsite of the alpha3beta2 nicotinic receptor. *J. Biol. Chem.* **2010**, *285*, 12355–12366. [[CrossRef](#)] [[PubMed](#)]
40. Luo, S.; Zhangsun, D.; Wu, Y.; Zhu, X.; Hu, Y.; McIntyre, M.; Christensen, S.; Akcan, M.; Craik, D.J.; McIntosh, J.M. Characterization of a novel alpha-conotoxin from *Conus textile* that selectively targets

- alpha6/alpha3beta2beta3 nicotinic acetylcholine receptors. *J. Biol. Chem.* **2013**, *288*, 894–902. [[CrossRef](#)] [[PubMed](#)]
41. Sali, A.; Blundell, T.L. Comparative protein modelling by satisfaction of spatial restraints. *J. Mol. Biol.* **1993**, *234*, 779–815. [[CrossRef](#)] [[PubMed](#)]
 42. Dutertre, S.; Ulens, C.; Buttner, R.; Fish, A.; van Elk, R.; Kendel, Y.; Hopping, G.; Alewood, P.F.; Schroeder, C.; Nicke, A.; et al. Achbp-targeted alpha-conotoxin correlates distinct binding orientations with nachr subtype selectivity. *EMBO J.* **2007**, *26*, 3858–3867. [[CrossRef](#)] [[PubMed](#)]
 43. Zouridakis, M.; Giastas, P.; Zarkadas, E.; Chroni-Tzartou, D.; Bregestovski, P.; Tzartos, S.J. Crystal structures of free and antagonist-bound states of human alpha9 nicotinic receptor extracellular domain. *Nat. Struct. Mol. Biol.* **2014**, *21*, 976–980. [[CrossRef](#)] [[PubMed](#)]
 44. Pronk, S.; Pall, S.; Schulz, R.; Larsson, P.; Bjelkmar, P.; Apostolov, R.; Shirts, M.R.; Smith, J.C.; Kasson, P.M.; van der Spoel, D.; et al. Gromacs 4.5: a high-throughput and highly parallel open source molecular simulation toolkit. *Bioinformatics* **2013**, *29*, 845–854. [[CrossRef](#)] [[PubMed](#)]
 45. Lindorff-Larsen, K.; Piana, S.; Palmo, K.; Maragakis, P.; Klepeis, J.L.; Dror, R.O.; Shaw, D.E. Improved side-chain torsion potentials for the amber ff99sb protein force field. *Proteins* **2010**, *78*, 1950–1958. [[CrossRef](#)] [[PubMed](#)]



© 2018 by the authors. Licensee MDPI, Basel, Switzerland. This article is an open access article distributed under the terms and conditions of the Creative Commons Attribution (CC BY) license (<http://creativecommons.org/licenses/by/4.0/>).